JTTEE5 9:225-234

Diagnostics and Modeling of an Argon/Helium Plasma Spray Process

Z. Duan, L. Beall, J. Schein, J. Heberlein, and M. Stachowicz

(Submitted 3 March 1999; in revised form 6 December 1999)

The natural instability of the arc in direct current (DC) plasma torches used in spray processing is one of the most important causes for variations in heating of sprayed particles, leading to inconsistencies in the final coating quality. A relatively simple diagnostic system has been set up to monitor the plasma jet instability, as well as some important process characteristics. Effects of the operating parameters and the anode condition on properties of plasma jets, particle properties, and coatings have been measured. These results show that the inconsistency caused by the jet instability influences the plasma spray process in several ways. The coating porosity and the deposition efficiency can be correlated to an average jet length obtained from a series of high speed images. Selected frequency peaks in the power spectrum of the acoustic signal are correlated with the average jet length, and these results are used to derive a simple control scheme, which adopts a fuzzy look-up model indicating the condition of the anode. Increasing the are current is the most effective way to counteract the negative effects of anode erosion.

Keywords plasma spray, diagnostics, control, modeling

1. Introduction

While plasma spraying has been a widely used technology over the past decades, few inexpensive yet effective diagnostics and controls are implemented for the industry. Most of the recent work in the diagnostics and control realms focuses on detection of properties of particles, which are being sprayed.[1–4] However, the variations in sprayed particle properties mainly result from the plasma jet instability. Such influences of the plasma jet instability on the coating process have been recently described.[5,6] In this paper, results of an investigation are presented, which describe the effects of the operating parameters and the anode condition on the measurable process characteristics associated with each component of the spray process.

Basically, the plasma spraying process can be divided into four components: the electric arc, the plasma jet, the particles in flight, and the coating. The word "plasma" usually represents the combination of the arc and the jet, but for diagnostics and control purposes, they must be distinguished. The characteristics of these components are not only controlled by operating parameters, such as current, gas flow rate, powder feed rate, standoff distance, *etc.*, but also strongly affected by factors, which are less controlled, such as surface condition of the anode, entrainment of ambient air into the jet, *etc.* Furthermore, the characteristic of each mentioned component influences all the following phases. For example, the trajectory and temperature of the particles in-flight may be significantly modified by the fluctuations of the plasma jet even for constant operating parameters, with corresponding variations in the coating properties. A schematic of the relationship between these components is shown in Fig. 1. In the first part of this paper, experimental measurements are described, which define relationships between properties of these components. The measurement results presented here include arc voltage, jet acoustic signal, jet appearance (length and width), in-flight particle properties (temperature and velocity), and coating properties (deposition efficiency and porosity).

If the relationship and interactions between these spray process components were completely understood, a control system could be developed, which would allow highly reproducible coatings for given operating conditions. However, one of the main difficulties in designing feedback diagnostics and controls for plasma spraying is that the real process is highly complex, nonlinear, and with uncertain causal relations. Because of the complexity and nonlinearity of the plasma spray system, empirical fuzzy logic models are used to simulate parts of the plasma system and provide insights into the spray process. In the second part of this paper, the fuzzy logic models and their use in the interpretation of experimental results are described. In the fuzzy logic models, the anode condition is considered as the uncontrolled variable and the average jet length as the parameter to be controlled. Fuzzy models are created to relate the current operating conditions and the inputs from sensors monitoring the system to determine both the condition of the anode and the quality of the coatings.

All experimental results and the fuzzy logic models presented in this paper are obtained with argon/helium mixtures as the plasma gas for specific torch configurations. Using a different gas or gas mixture rather than argon or argon/helium might result in different plasma dynamic characteristics, and the models may no longer be able to precisely describe the process characteristics; however, it is well expected that similar dependencies will exist in all the direct current (DC) plasma spray systems.

Z. Duan and **J. Heberlein,** Department of Mechanical Engineering, University of Minnesota, Minneapolis, MN 55455; **L. Beall,** Praxair Surface Technologies, Appleton, WI 54912; **J. Schein,** Alameda Applied Sciences Corp., San Leandro, CA 94577; and **M. Stachowicz,** Department of Electrical and Computer Engineering, University of Minnesota-Duluth, Duluth, MN 55812.

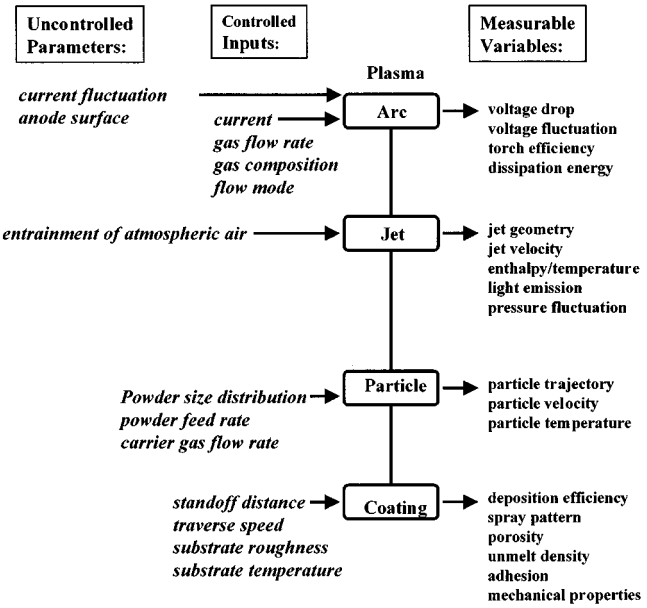

Fig. 1 Diagram of the plasma spray process stages

2. Experimental Setup and Conditions

The investigations presented in this paper have been carried out with a Praxair SG-100 (Praxair Surface Technologies, Appleton, WI) plasma spray torch operating in the subsonic mode with anode #2083-720 and cathode #1083-720. Three different gas injectors have been used to achieve different vortex strengths in the arc gas flow. Praxair #3083-113 and #3083-112 have been used to obtain a full swirl flow and a full straight flow, respectively. The third, custom-made gas injector can produce a flow condition with a 20% swirl component and an 80% straight flow component. The plasma gas is an argon/helium mixture, with a fixed total flow rate of 60 slm. The sprayed powder is Praxair ZRO-113/114, which is 8 wt.% yttria, partially stabilized zirconia with a size range of –106/+45 μm. The standoff distance of the substrate for spraying is set at 10 cm from the nozzle exit, and the measurements of the particle properties are also performed at this position. The operating parameters of the torch are varied in each test run to obtain data for an experimental matrix. The parameters, which are varied, include are current, plasma gas composition (*i.e.*, ratio of helium to argon), and gas flow mode. The ranges of the parameter values are listed in Table 1. Anode erosion has been identified as the uncontrolled parameter. All experiments have been performed with three different anodes, each having various degrees of service time and surface erosion, as listed in Table 2.

Coatings are primarily deposited on $50 \times 25 \times 2$ mm mild steel substrates. These substrates are prepared by ultrasonic cleaning to remove grease or machine oil deposits and grit blasting to roughen the surface before spraying. The substrate is mounted on a rotating disk, orthogonal to the torch center line, and repeatedly travels past the particle plume with a speed of 85 cm/s. The coatings are formed on the substrate over a 2 min spraying period without additional substrate cooling or preheating.

After the deposition, the substrates with coating have been cut and mounted using a cold setting epoxy and the cross sections polished for microscopic examination. Metallographic examination is carried out with an optical microscope and a computerized image analysis system. Coating porosity serves as the primary indication of the coating quality. The deposition efficiency of the spray system is also determined to reveal the torch performance. The results are obtained by measuring the fraction of the mass, which is deposited when spraying on a rotating plate.

Table 1 Plasma torch operating conditions

Parameters	Settings
Arc current	700 to 900 A
Gas mixture	Ar/He: 60/00, 48/12, and 40/20 slm
Gas flow	Straight, 20% vortex, and 100% vortex

Table 2 Tested anode conditions

Anode	Ignition times	Service time	Depth of erosion
New	<50	<10 h	<0.2 mm
In use	~200	~20 h	0.4 mm
Bad	Burnt due to cooling failure		1.4 mm

The LaserStrobe™ video system made by Control Vision Inc. (Idaho Falls, ID) has been used to examine the plasma jet appearances in the plasma spray process. The images, obtained with a high shutter speed (50 or 100 ns) CCD camera, are transferred to a computer with a frame grabber and stored on videotape. In the real time acquisition case, the maximum sampling rate is 15 frames per s. These images are processed using customized NIH Image software (National Institute of Health, Bethesda, MD), which provides information about the plasma jet, such as the jet length and the jet width. These parameters are computed as the average value from 10 to 40 video frames of the jet.

The in-flight properties of the sprayed particles are measured using the DPV-2000™ system obtained from TECNAR Automation Ltd. (Montreal, Canada), which uses infrared pyrometry along with a dual slit arrangement for time-of-flight measurements on individual particles. The system can provide velocity, temperature, and size measurements of up to 220 individual particles per second. The sensor head is mounted on a X-Y scanner, which can move the measurement volume in both horizontal and vertical directions. To obtain a two-dimensional distribution of the measured particle properties, the measurement volume has been moved on the surface, which is perpendicular to the nozzle axis with an axial location at the mentioned standoff distance. For each operating condition, the measurement is performed along a matrix of 9×9 points with a point-to-point distance of 5 mm. The system samples data for 5 s at each measuring point. To avoid random errors, the measurements at any measuring point will be treated as no effective data if the system cannot cumulatively capture more than 30 particles in the 5 s period.

The acoustic signals are captured by a microphone with an audio amplifier. The microphone has a smooth frequency response in the 20 to 20,000 Hz range. The microphone is directed toward the torch nozzle exit and installed in a sound-insulating tube to prevent the capture of off-axis acoustic signals. Furthermore, sound-absorbing foam is positioned on the other side of the plasma jet from the microphone to prevent the wall of the spray booth from echoing the plasma noise into the microphone and creating interferences.

Both voltage and sound signal are collected by a Hewlett-Packard 54540A (Hewlett-Packard, Colorado Springs, CO), four channel oscilloscope which is remotely controlled by a computer using the LabVIEW™ (National Instruments, Austin, TX) software through a GPIB cable. Along with the amplified acoustic signal, the arc voltage is sampled with the oscilloscope using a 10X probe. Each signal contains 4096 points with a sampling rate of 50 kHz and can be real time processed and stored in the computer. LabVIEW™ software can conveniently perform spectral analysis and mean and standard deviation calculations. For one set of data (ten acquisitions), the time for a simple processing procedure (sampling 4096 data points, fast Fourier transform, and displaying the results) is less than 30 s. A detailed discussion of the signal analysis can be found in Ref 7 and 8.

3. Experimental Results

3.1 Jet Appearances

Figure 2 shows a typical plasma jet appearance obtained using the LaserStrobe™ video system with a shutter time of 50 ns. The jet length and the jet width are considered as the primary characteristics of the jet appearance. However, the results of the jet length and width measurement would change if the setup of the video system varies, since the output images are obtained through an optical aperture and a gain-adjustable CCD camera. Therefore, for all the experiments being performed, the aperture in the optical system and the sensor gain for the CCD camera are fixed so that relative comparisons among the different operating conditions can be performed. Furthermore, the jet length and the jet width data presented here are obtained by averaging 40 images.

Figure 3 shows the dependence of the average jet length and the average jet width on the arc current with the new anode and the bad anode. The results are obtained with full swirl flow and a plasma gas flow rate of 48/12 slm of argon/helium. The jet length and the jet width almost linearly increase with increasing arc current, since the energy dissipation of the arc rises with the increasing current. With the current rising from 700 to 900 A, the jet length increases from 27 to 37 mm with a new anode and from 22 to 29 mm with a bad anode, respectively. The jet width shows the same trend. On the other hand, the jet lengths and widths with a bad anode are obviously smaller than those with a new anode. With the same current, the jet lengths and the jet widths with a new anode are about 20 to 25% higher than those with a bad anode. The main reason for this result is that the arc with an eroded anode is shorter and more unstable compared to the one with a new anode; thus, the average voltage and the dissipated power are smaller with the eroded anode.

As shown in Fig. 4, increasing the helium fraction in the arc gas can also increase the jet length and width. The dependence of the jet length and width on the helium fraction is obtained with full swirl flow and an arc current of 800 A. The helium increases the thermal conductivity of the plasma gas, therefore leading to a higher arc voltage. However, the effects of the helium are strongly reduced when the anode is seriously eroded. The jet width increases from 4.2 to 5.2 mm with the new anode, while it only changes from 3.9 to 4.1 mm with the bad anode. The jet length shows the same characteristic. Since the addition of helium only changes the arc gas properties in a limited range, the arc will keep fluctuating between the well-defined spots in a

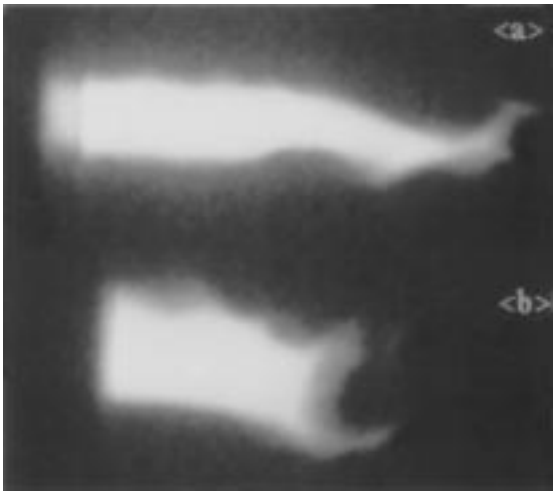

Fig. 2 Plasma jet appearance obtained using a 50 ns shutter time: (**a**) with a new anode and (**b**) with a bad anode.

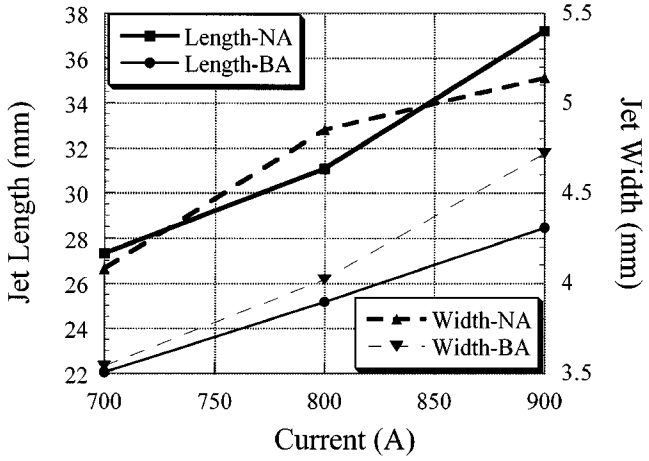

Fig. 3 Jet length/width dependence on the arc current with a new anode (NA) and a bad anode (BA)

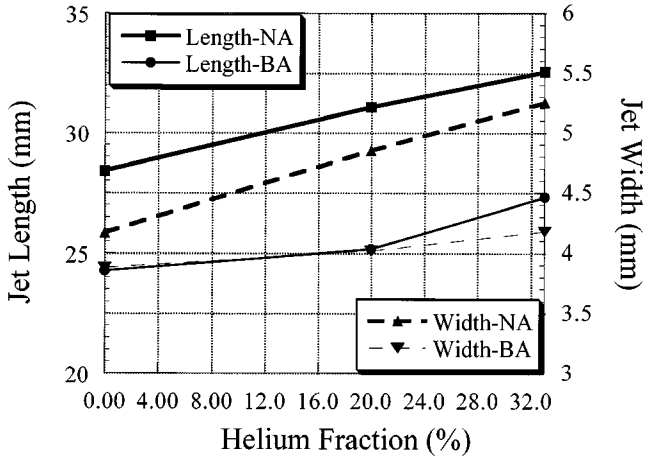

Fig. 4 Jet length/width dependence on the helium fraction with a new anode (NA) and a bad anode (BA)

strongly eroded anode; thus, the average voltage and energy dissipation are more influenced by the erosion features of the anode than by the helium addition.

3.2 In-Flight Particle Properties

The results obtained using the DPV-2000 system can be presented in the format of a contour plot, which shows the distribution of the measured variables on the scanning surface in a plane at a certain axial distance from the nozzle, as shown in Fig. 5 and 6. The measured variables here are measured number of particles, particle temperature, particle velocity, and particle size. The temperature, the velocity, and the size are average values computed over the total number of measured particles at each position. The data for particle sizes are obtained using a single calibration factor without recalibration for different conditions. Therefore, the presented particle sizes are not the real particle sizes but can be considered proportional to the real ones, and provide relative comparisons. Figure 5 shows the results obtained with the new anode and Fig. 6 with the bad anode, both obtained at an axial location 10 cm downstream from the nozzle exit, with full swirl argon/helium flow and a flow rate of 40/20 slm, and a current of 900 A.

From both figures, it can be found that the particles are slightly separated according to their size, because the large momentum of the heavy particles makes them penetrate the viscous plasma jet deeper compared to the small particles. The position where the maximum temperature occurs does not match that of the maximum velocity. The fastest velocities appear, as expected, with the lighter particles, while the highest temperatures are approximately at the center of the measured particle distribution pattern. However, comparing Fig. 6 with 5, some of the effects of the anode erosion can be seen. The maximum and average values of the particle temperatures and velocities with a strongly eroded anode are lower than those with a new anode. Furthermore, the particle number distribution in Fig. 6 shows a wider and more symmetric distribution pattern, consistent with the fact that the anode erosion enhances the fluctuations in particle heating and acceleration, by increasing the jet instability, and reduces the influences of swirl flow, by forcing the arc to fluctuate between well-defined spots.

The contour plots such as Fig. 5 and 6 are too complex when large amounts of data need to be compared. In this case, a convenient method is to use the weighted average temperatures and velocities. These values are obtained in the following way: multiplying the number of particles and the average temperature

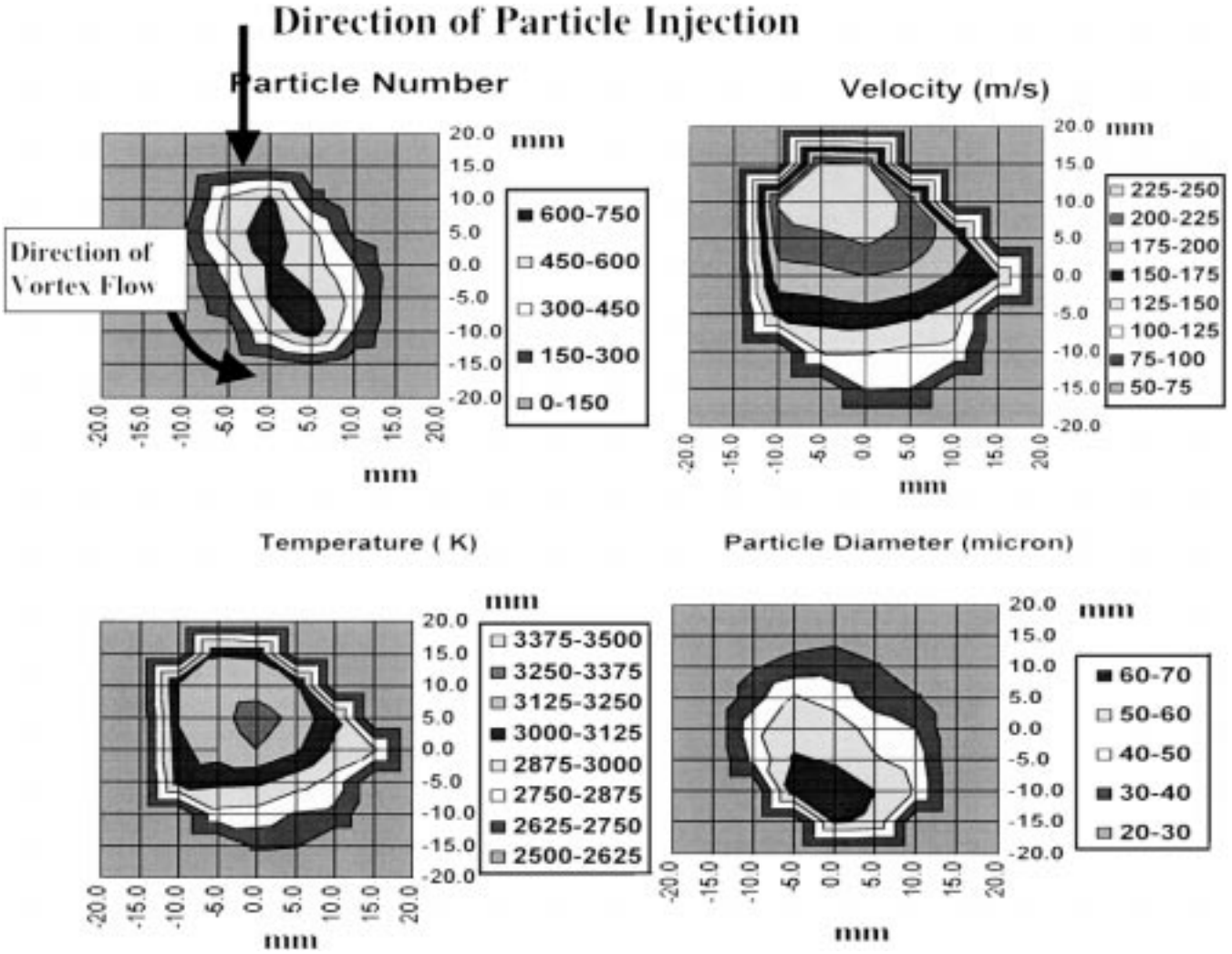

Fig. 5 Sprayed particle property distributions for a new anode

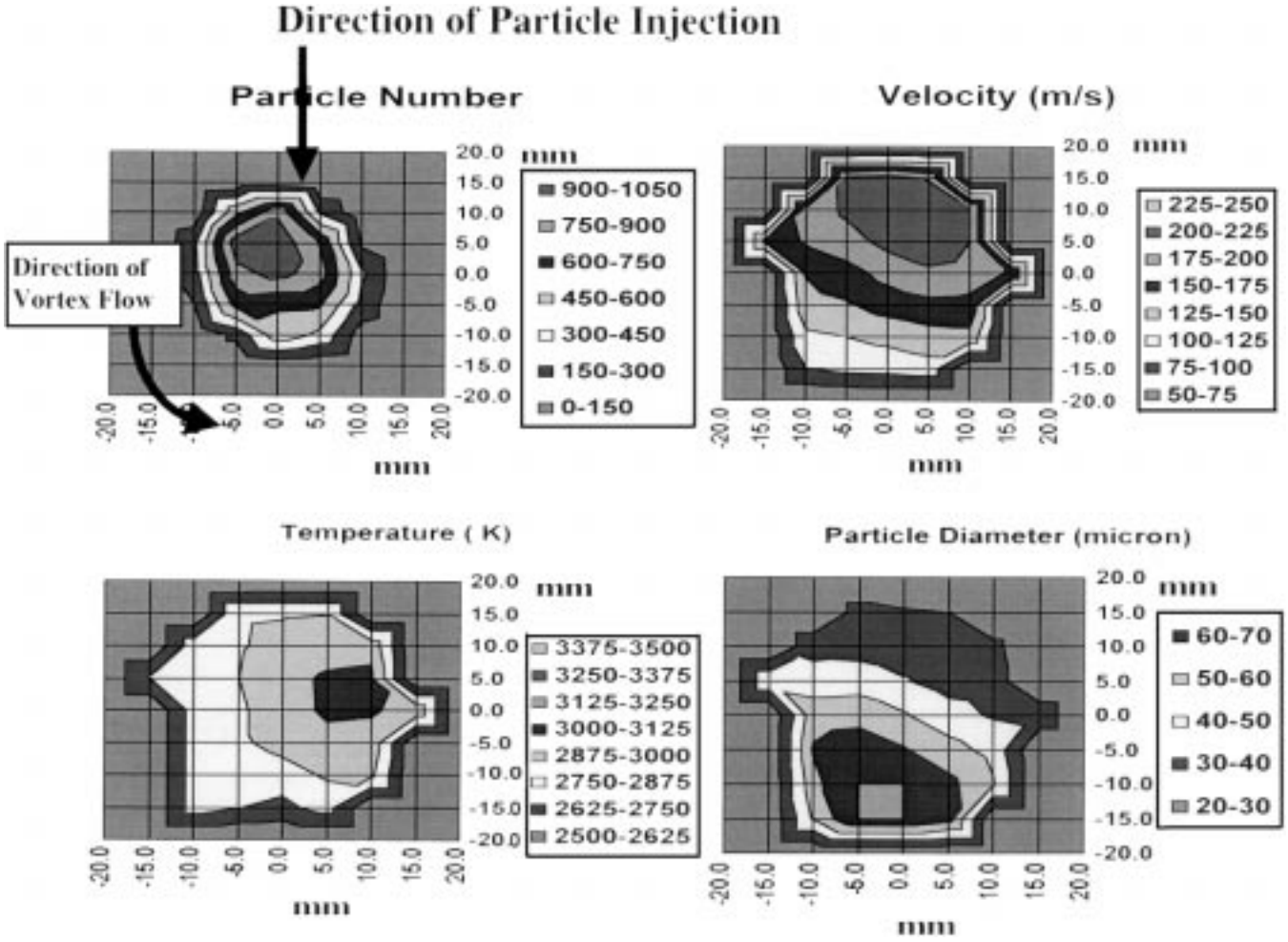

Fig. 6 Sprayed particle property distributions for a bad anode

or velocity for each measuring position, summarizing these products and dividing the sum by the total number of particles counted. In the following paragraphs, the effects of the operating conditions on the particle properties—mainly temperature and velocity—will be discussed. All results presented refer to the weighted, average values, and are obtained at an axial distance of 10 cm downstream from the nozzle exit. It should be noted that the DPV-2000 system has a limit in detecting low particle temperatures, so a lower-weighted average temperature means that there are more particles below the system detection limit, which may not be molten.

An increasing current raises the operating power level of the plasma torch, and therefore raises the particle temperatures and velocities, as shown in Fig. 7. The results presented in Fig. 7 are obtained with full swirl flow and an argon/helium gas flow of 48/12 slm. The particle temperatures and velocities increase almost linearly with increasing currents with all of the anodes investigated, but anode erosion decreases the particle temperatures and velocities basically by decreasing the plasma jet length and width. A strongly eroded anode reduces the average particle temperature value by up to 150 °C and the velocity value by up to 10 m/s.

The relative amount of helium influences the particle properties as it influences the jet length and width. Figure 8 shows the dependence of the particle average temperatures and velocities on helium flow rates with different anodes, obtained with full swirl flow and a current of 800 A. Consistent with the results for the jet length and width, the particle temperatures and velocities increase with more helium in the plasma gas. But increasing helium flow also shows a reduced effect on particle properties when the anode is strongly eroded.

By changing the gas injector, the plasma gas flow characteristics are changed, which also strongly influences the particle properties. Figure 9, obtained with an arc current of 800 A and an argon/helium plasma gas flow rate of 48/12 slm, shows the influence of the gas flow mode on the particle properties. An increasing vortex strength will constrict the arc column, thus raising the are voltage and operating power level, and increase the particle temperatures and velocities. Here, the negative effects of anode erosion on the particle properties are shown again. It should be noted, however, that increasing the percentage of vortex flow beyond 20% does not provide any further increase in average particle temperature and velocity.

3.3 Coating Properties

Similar trends as those found in the plasma jet characteristics and the particle properties can be seen in the influence of

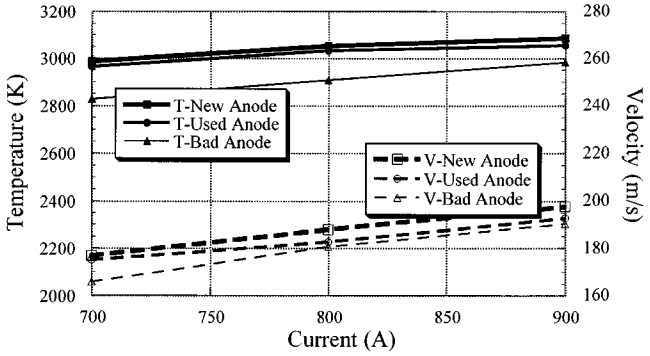

Fig. 7 Dependence of the average particle temperature (T) and velocity (V) on the arc current with a new anode, a used anode, and a bad anode

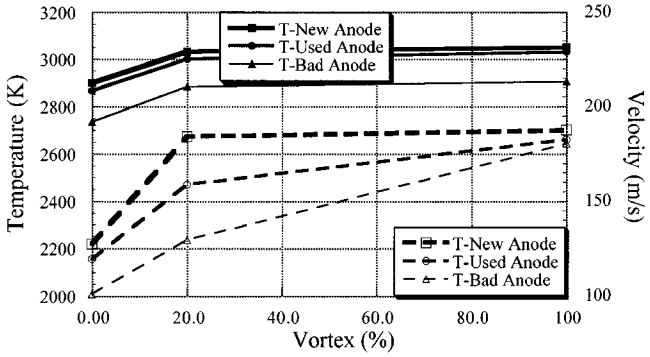

Fig. 9 Dependence of the average particle temperature (T) and velocity (V) on the vortex strength with a new anode, a used anode, and a bad anode

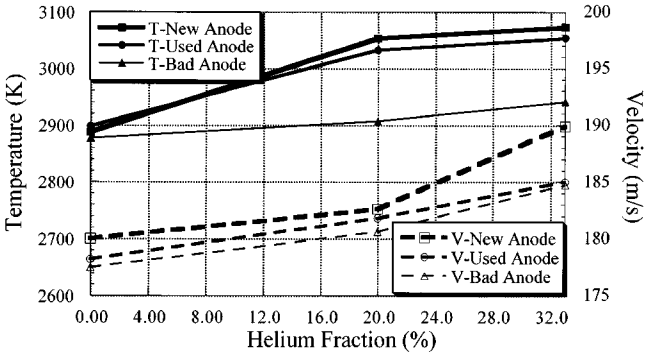

Fig. 8 Dependence of the average particle temperature (T) and velocity (V) on the helium fraction with a new anode, a used anode, and a bad anode

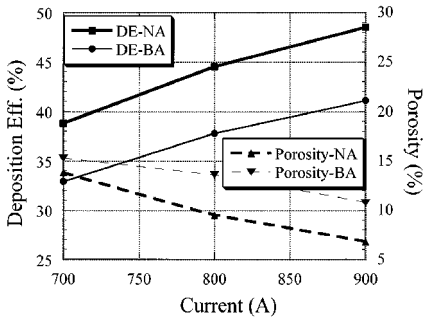

Fig. 10 Dependence of the deposition efficiency and coating porosity on the arc current with a new anode (NA) and a bad anode (BA)

the operating parameters and the anode conditions on the coating qualities. Figure 10 shows the effect of the arc current, Fig. 11 the effect of the percentage of helium in the plasma gas, and Fig. 12 the effect of the flow mode (vortex strength). They are obtained with the new anode and the bad anode using full swirl flow mode (except Fig. 12), a flow rate for argon/helium mixture of 40/20 slm (except Fig. 11), and a current of 900 A (except Fig. 10).

An improvement in the coating qualities, which means an increasing deposition efficiency and a decreasing coating porosity, occurs either with a high operating current or with a high concentration of helium in the plasma gas. The addition of helium has a stronger effect with a new anode than with a strongly eroded anode. The vortex also increases the deposition efficiency and decreases the coating porosity by constricting the arc column, thus leading to higher arc voltages and operating power levels. It is interesting to note that while the average particle temperatures and velocities are not strongly influenced by increasing the fraction of vortex flow above 20%, the coating properties are affected by the increase.

4. Fuzzy Model

In previously reported results[5,9] the arc voltage and the sound signal obtained with a microphone have been shown to provide similar information about the state of the plasma spray system, but the sound signal seems to provide some additional information, which cannot be found in the voltage signal. Because of this, the sound signal is selected as an indicator of the plasma torch performance.

The power spectra of the sound (and voltage) signals show groups of peaks in certain frequency ranges, which seem to follow distinct patterns depending on the condition of the anode. For instance, the power spectrum of the sound signal typically has two groups of peaks: one in the range from about 4 to 8 kHz and another in the range from 8 to 12 kHz. The first peak mirrors the principal frequency of the voltage fluctuations and is therefore likely related to the arc length and are power variations. The second peak is probably related to large-scale turbulence. Comparisons of the widths and relative heights of this range of peaks have been used to give an indication of the condition of the anode and the character of the plasma jet.

4.1 Model Description

While the phenomenon mentioned above is easy to identify visually in the power spectrum of the sound signal, it is difficult to quantify. This quantification is obtained with the aid of functions, which are part of the LabVIEW™ software. Using these functions, an average of ten spectral samples of the sound signal is calculated. The voltage fluctuation frequencies due to the

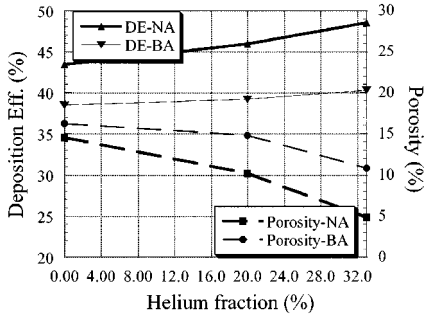

Fig. 11 Dependence of the deposition efficiency and coating porosity on the helium fraction with a new anode (NA) and a bad anode (BA)

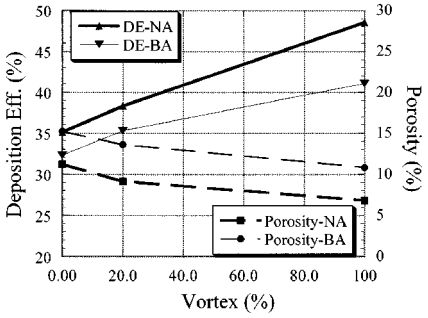

Fig. 12 Dependence of the deposition efficiency and coating porosity on the vortex strength with a new anode (NA) and a bad anode (BA)

power supply are eliminated with a high pass filter with a cut-off frequency of 2 kHz.

To identify the frequency ranges of the characteristic peaks, two fifth degree polynomial functions are fitted to the filtered spectral data to describe two central peaks. The first function maps the data up to 8 kHz, and the second function maps the data from 8 kHz and above. In addition, the width for each of the peaks is calculated by locating the points on the polynomial function, where the function has a value equal to 0.75 times the height of the peak. Figure 13 shows an example of the processed sound signal containing the filtered power spectrum, the two fitting polynomial functions, the two peaks indicated by the dots, and the widths represented by the horizontal lines. The sound peak ratio discussed later is the ratio of the height of the first to that of the second peak.

The sound signals are processed on-line and simultaneously with the images captured by the LaserStrobe™ video system providing information about jet geometries. In particular, comparisons are obtained with the average jet length for each of the operating conditions. As shown in the previous section, there is a strong correlation between this jet property and the coating quality. Consequently, correlation of the sensor measurements with these values gives a way to indirectly evaluate coating properties during runtime.

Since the plasma spraying process is nonlinear and very complex, fuzzy logic models have been used to help interpret the data collected during experimentation. A fuzzy logic model uses linguistic rules to describe the correlation between input and output variables. In the plasma spray system, a typical fuzzy logic

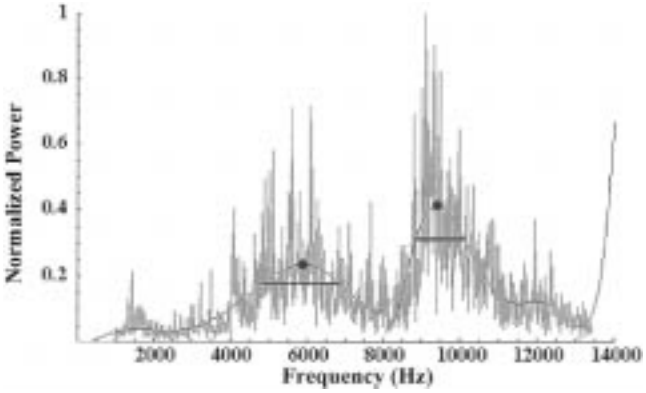

Fig. 13 Processed acoustic spectrum

rule might look like the following (Ref 10): IF Arc Current is *Medium* and Total Flow Rate is *Low* and Ar/He Ratio is *Average* and Sound Peak Ratio is *Large*, THEN Anode Condition is *Poor*. The linguistic terms in fuzzy logic rules are described using membership functions. For each variable, which is described in a fuzzy logic system, membership is graded to any value in the normal operating range of the variable. Figure 14 shows the membership functions, which have been used to describe the variables for this project.

Since the ranges of the input and output variables for the systems are well known, a Table Look-up Method (Ref 10) has been used for designing the fuzzy system. This method uses input-output data from a process to create a fuzzy model of the process. With knowledge of the typical ranges of the operating parameters, an informative linguistic description of the variables involved has been created. In modeling parts of the plasma spray system, two fuzzy models have been created. The first model relates input data containing the operating conditions and sound information to the condition of the anode. The second fuzzy model relates the operating conditions and sound information to the arc length.

4.2 Sound Peak Ratio as an Indicator of Anode Conditions

The first fuzzy system has been created from a data set containing four input, the arc current, the total flow rate, the Ar/He ratio, and the ratio of the peaks in the sound spectrum (Fig. 14), and one output, the condition of the anode. In the data set, the condition of the anode is represented by a number that ranged from 0 to 10, where 0 represents a very poor anode and 10 represents a brand new anode.

This model is a four input, one output system, so it is difficult to display the results on a single graph. One way to visualize the results is to keep some of the inputs constant and plot the model with the other variables allowed to vary. Figure 15 shows the results of plotting the *Anode Condition* as a function of the *Arc Current* and the sound *Peak Ratio*. In this plot, the total flow rate is kept constant at 60 slm, and the Ar/He ratio is 4 to 1; these are the typical operating conditions used with our torch. The high areas of the graph indicate points where the anode condition is good, and the low points show areas consistent with a poor anode condition.

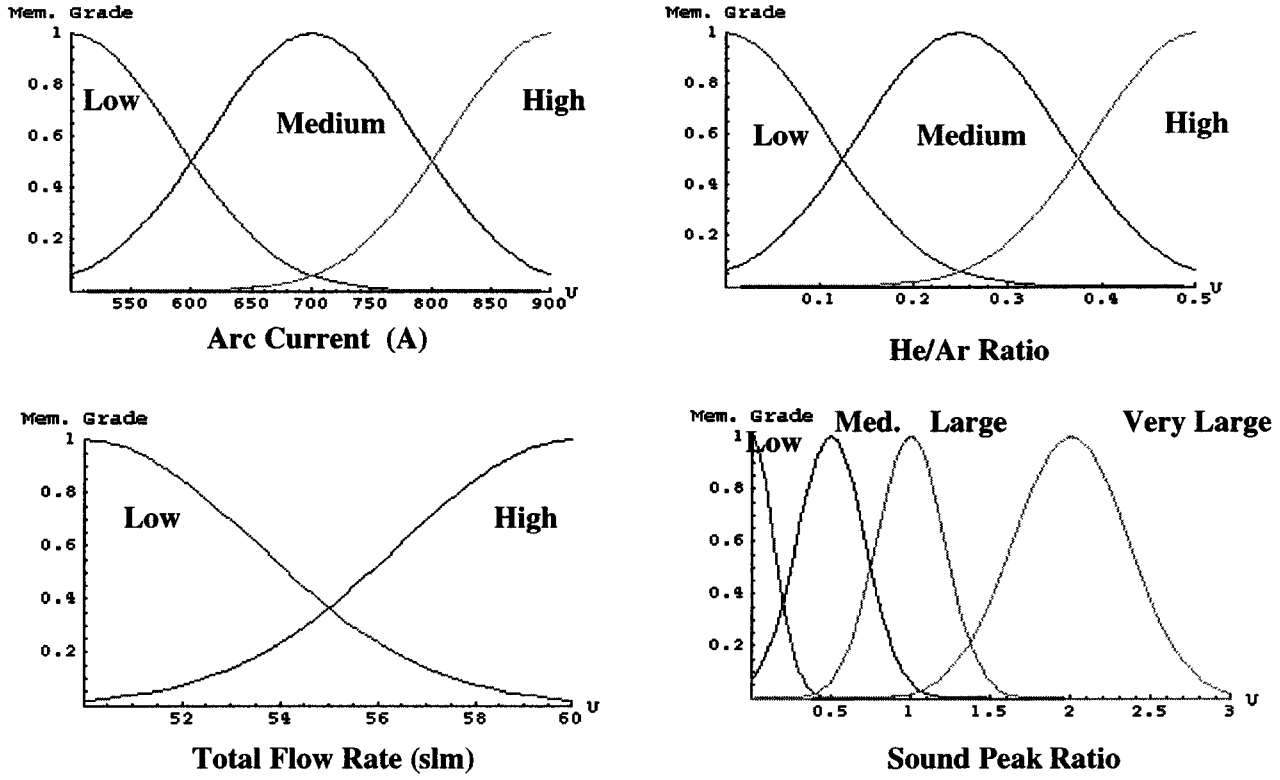

Fig. 14 Membership functions used in the fuzzy logic model

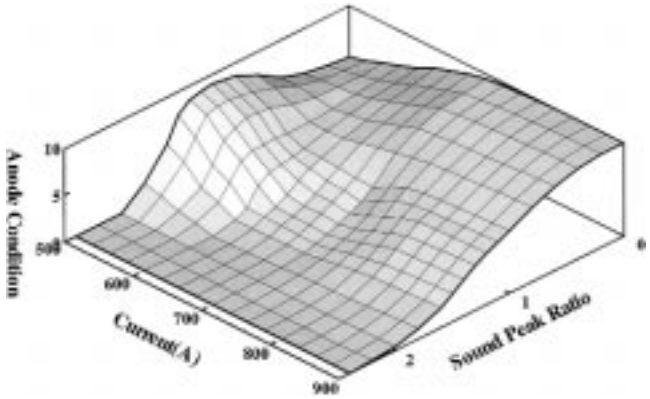

Fig. 15 Anode condition as a function of sound peak ratio and current

From Fig. 15, it can be seen that the ratio of the sound peaks is a clear indication of the anode condition for are currents of 600 A or above; at lower currents, the indication is less clear. From Fig. 15, it is clear that small sound peak ratios are indicative of a new or good anode. Conversely, high sound peak ratios (1 and above) indicate an anode in poor shape. This information can be put to use for devising a feedback control system for a plasma spray process.

4.3 Counteracting Anode Erosion

The second fuzzy models relate the input parameters to the average length of the plasma jet. Figure 16 shows a series of graphs plotting the average length of the plasma jet as a function of the He/Ar ratio and the are current. In the series of graphs, the sound peak ratio is allowed to range from 0.5 in the first graph to 1 in the second graph to 2 in the final graph. Based on the results from Fig. 15, the conditions shown in the graphs in Fig. 16 are consistent with a good anode, a used anode, and a poor anode, respectively.

From the first graph in Fig. 16(a), it can be seen that for an anode in good condition, the average jet length can be increased, by increasing the arc current or the He/Ar ratio. In Fig. 16(b), it can be seen that the current still has a strong influence on the average jet length, but the He/Ar ration has less of an effect. Finally, in Fig. 16(c), we see that the He/Ar ratio has little affect on the jet length, and only very high currents produce high jet lengths.

Based on the observations made from the models above, a feedback control system is proposed for stabilizing the average arc length of the plasma jet. The control system uses the measurement of the average jet length as a feedback variable. The control system compares this value to the desired jet length and performs the control based on the error. Information about the current state of the anode, given by the sound peak ratio, provides additional information to the controller. The anode condition information can be used to scale parameters in the feedback controller, or the anode condition information could be used to select a controller, which is tuned for the particular state of the anode.

Based on the modeling information shown earlier (Fig. 15 and 16), the feedback controller could be some sort of Proportional-Integral-Derivative controller for cases when the anode is

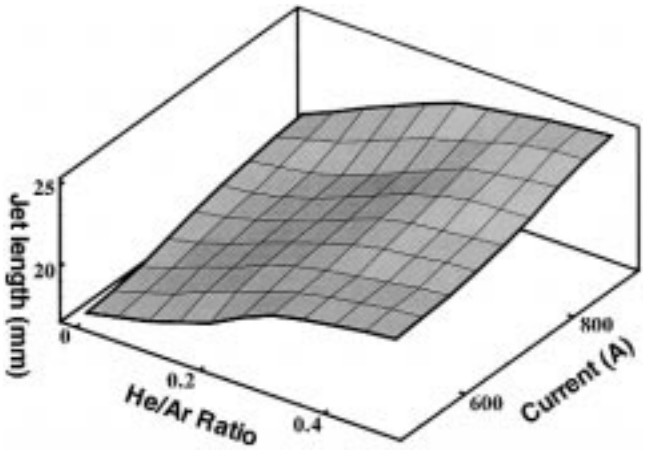

(a)

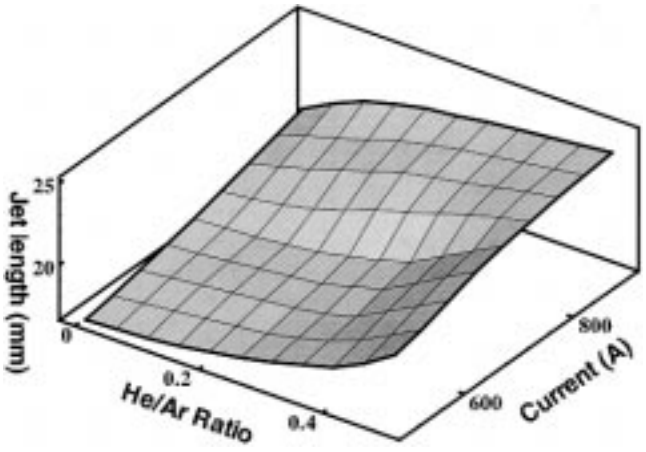

(b)

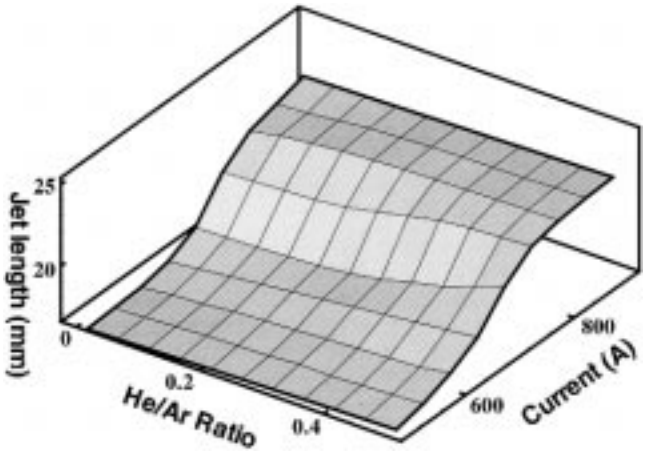

(c)

Fig. 16 Jet length models (**a**) for a new anode, (**b**) for a used anode, (**c**) for a bad anode

still in relatively good shape, since two control variables (current and argon/helium ration) need to be adjusted. The controller can simply increase the current (or the He/Ar ratio) when the jet length error is positive and decrease the current (or the He/Ar ratio) when the jet length error is negative. As the condition of the anode worsens, the control would be performed using only the arc current, and the scaling of the controller would have to change.

5. Conclusions

Using a simple diagnostic system for monitoring the plasma spray process, experimental results on jet appearances, in-flight particle properties, and coating qualities with various operating conditions and anode wear levels have been obtained. The measured results are used to establish the relationships between the spray process components. With increasing currents and secondary gas flow rates, the coating qualities can be improved due to a longer plasma jet and better heating of sprayed particles. This observation allows us to achieve an on-line diagnostic, which predicts the coating quality by monitoring the properties of the plasma jet. However, the anode condition affects jet, particle, and coating properties even for constant operating parameters. A strongly eroded anode significantly reduces the jet length, thus resulting in reduced particle heating and increased coating porosity. Accordingly, different anode conditions require a different set of values for the operating parameters for optimal torch operation.

Based on experimental observations and frequency analysis, the power spectrum of the acoustic signals associated with the spray torch appears to be the most appropriate process indicator. With a system requiring a microphone and a personal computer, a simple fuzzy model can be used to describe the effects of the operating parameters on the jet lengths with different anode conditions. The fuzzy model can also provide a strategy to on-line monitor the anode condition using acoustic spectra, thus adjustments to counteract the anode erosion. This strategy can serve as the basis of a feedback control system, which stabilizes the average length of the plasma jet. Although the results in this paper are obtained with a specific torch, the evolution of the various parametric dependencies should apply to most DC plasma spray torches. In particular, it is believed that sound peak ratios and jet lengths can be related to anode condition and coating porosity, and can thus be used as process control variables.

Acknowledgment

This work has been supported, in part, by the University of Minnesota through the Center for Advanced Control for Plasma Processing and by the National Science Foundation through the Engineering Research Center for Plasma-Aided-Manufacturing, grant No. EEC-87-21545. The government has certain rights in this material.

References

1. C. Moreau, P. Gougeon, M. Lamontague, V. Lacasse, G. Vandreuil, and P. Cieto: in *Thermal Spray Industrial Applications*, C.C. Berndt and S. Sampath, eds., ASM International, Material Park, OH, 1994, pp. 431-37.
2. W.D. Swank, J.R. Fincke, and D.C. Haggard: in *Thermal Spray Science & Technology*, C.C. Berndt and S. Sampath, ed., ASM International, Materials Park, OH, 1995, pp. 11-16.

3. M. Prystay, P. Gougeon, and C. Moreau: in *Thermal Spray: Practical Solutions for Engineering Problems*, C.C. Berndt, ed., ASM International, Materials Park, OH, 1996, pp. 511-16.
4. R.N. Wright, J.R. Fincke, W.D. Swank, and D.C. Haggard: in *Thermal Spray: Practical Solutions for Engineering Problems*, C.C. Berndt, ed., ASM International, Materials Park, OH, 1996, pp. 517-24.
5. Z. Duan, L. Beall, M.P. Planche, J. Heberlein, E. Pfender, and M. Stachowicz: in *Thermal Spray: A United Forum for Scientific and Technological Advances*, C.C. Berndt, ed., ASM International, Materials Park, OH, 1997, pp. 407-11.
6. M.P. Planche, Z. Duan, O. Lagnoux, J. Heberlein, J.F. Coudert, and E. Pfender: *Proc. 13th Int. Symp. on Plasma Chemistry*, C.K. Wu, ed., Peking University, Beijing, 1997, pp. 1460-65.
7. Z. Duan: Master's Thesis, University of Minnesota, Minneapolis, MN, 1997.
8. S. Malmberg: Ph.D. Thesis, University of Minnesota, Minneapolis, MN, 1994.
9. L. Beall, Z. Duan, J. Schein, M. Stachowicz, M.P. Planche, and J. Heberlein: in *Thermal Spray: Meeting the Challenges of the 21st Century*, C. Coddet, ASM International, Materials Park, OH, 1998, pp. 815-20.
10. Li-Xin Wang: *A Course in Fuzzy Systems and Control*, Prentice-Hall, Upper Saddle River, NJ, 1997.